2009 American Control Conference
Hyatt Regency Riverfront, St. Louis, MO, USA
June 10-12, 2009

A Full Dynamic Model of a HVAC Vapor Compression Cycle Interacting with a Dynamic Environment

Bin Li, and Andrew G. Alleyne, *Senior Member, IEEE*

***Abstract*—This paper presents an advanced switched model approach for vapor compression cycle (VCC) systems with shut-down and start-up operations. Building upon recent work [2], a full dynamic system model with switched moving-boundary components is presented that is able to accommodate severe transients in heat exchanger dynamics. These new switched heat exchanger models are created with uniform model structures, but with combinations of different model representations. It is shown that switching schemes between different representations handle the transitions of dynamic states while keeping track of vapor and liquid refrigerant regions during stop-start transients. The dynamic system model is created in Matlab/Simulink and is successfully verified on an experimental test stand. A combined VCC/environment is simulated with a hysteretic temperature controller in a case study. The qualitative accuracy of the case study results demonstrate the potential for this dynamic switched model approach for controller designs, including compressor cycling, in VCC systems.**

I. Introduction

THE primary goal of any vapor compression cycle (VCC) system in the HVAC industry is to transfer energy from one location to another. Most VCC systems operate in a mode in which they stop and start the refrigerant flow in order to modulate the amount of cooling/heating capacity provided to some enclosed environment. Here, this is termed the 'compressor cycling', or *stop-start*, problem for dynamic VCC modeling and control.

It is a challenging task to balance the trade-offs between accuracy and complexity in the modeling of a VCC system to create an approach which is useful for both dynamic analysis and control designs. Two general paradigms are currently used in VCC system modeling: moving-boundary models and finite difference (spatially dependent) models [1]. The moving-boundary method is the method of choice over the finite difference method for controls' purposes because of its speed in real-time computer simulation [2]. Furthermore, the moving-boundary models provide industrial practitioners and control engineers with physical insights into the plant's dynamic behaviors [3].

In the moving-boundary modeling framework, the heat exchanger is divided into control volumes, or *zones*, in terms of fluid phase. The location of the boundary between zones is the key dynamic variable that captures the essential multi-phase flow dynamics. In [4][5], moving-boundary heat exchangers models were developed as low-order, control-oriented, dynamic system models. Within this framework, compressor cycling produces very large transients which result in the creation and destruction of dynamic states [6]. The main challenge for moving-boundary models of the VCC system is how to transition between full refrigerant flow, no flow, and back again to full flow condition. Previous work [7][8] applied model switching approaches to accommodate multiple modeling frameworks in one simulation. [7][8] presented multiple model structures for representing the switching requirement during transients. Willatzen et al. [8] described useful techniques for controlling inactive states during evaporator model switching, but no model validation results were presented. Most recently, McKinley et al. [2] developed an advanced switched system model for a single heat exchanger (condenser). *Pseudo-state* variables were introduced to accommodate the changing dynamic states during model switching. Another contribution of [2] is the presentation of novel switching schemes based on void fraction in order to ensure refrigerant mass conservation. As motivated by [2], this paper seeks to develop a full dynamic model for the VCC system using the switched model approach to capture the compressor cycling dynamics, one of the common capacity control methods in the HVAC industry. To the knowledge of the authors, this is the first report in the literature of a *stop-start* VCC cycle simulated with moving-boundary models.

The rest of the paper is organized as follows. Section II describes the new moving-boundary heat exchanger models developed using the framework in [2]. In particular, the switched evaporator model is developed with two *modes*, and the switched condenser model in [2] is extended to five *modes*. Switching criteria between different *modes* are specified for the dynamics of a *stop-start* cycle. Section III provides model validation results using a benchtop experimental system. The results demonstrate the capabilities of the models in Section II for capturing compressor cycling behavior. To illustrate the value of the *stop-start* cycle model, Sections IV and V integrate the VCC cycle with an enclosed environment and implement a baseline industrial controller. The environment model is presented and validated in Section IV, while Section V demonstrates the use of an industry standard hysteresis controller. A conclusion section summarizes the main points

Bin Li and A. G. Alleyne are with the Department of Mechanical Science and Engineering at the University of Illinois, Urbana-Champaign, 1206 West Green Street, MC-244, Urbana, IL, USA, 61801. (e-mail:binli2@illinois.edu; alleyne@illinois.edu; phone: 217-244-9993; fax: 217-244-6534)

of the paper.

II. Modeling of Switched Moving-Boundary Heat Exchangers

Using the framework in [2], a modeling approach for an evaporator with switched representations is presented in this section. Subsequently, a switched moving-boundary condenser is presented that extends the initial work of [2]. With both model sets, a full *stop-start* VCC cycle can be represented. The reader is encouraged to examine the Nomenclature for relevant variable definitions. Also, more information about the modeling approach and assumptions can be found in [2].

A. Switched Moving-Boundary Evaporator Model

For an idealized VCC cycle, the refrigerant entering the evaporator is a saturated liquid-vapor mixture. The refrigerant leaving the evaporator ranges from a superheated vapor to a saturated liquid-vapor mixture through different operating conditions. Assuming the *stop-start* transition dynamics to be 'full refrigerant flow; no flow; full flow again', two different evaporator representations are needed. These are a two-zone model *mode 1* and a one-zone model *mode 2* as illustrated in Fig. 1.

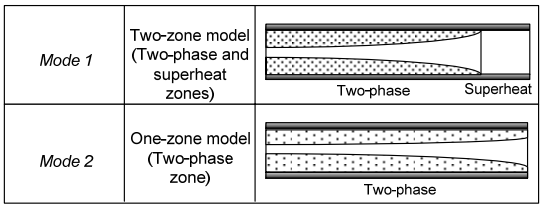

Fig. 1. Switched moving-boundary evaporator model structure

The dynamic state vector in (1) represents the evaporator conditions at each instant time, independent of model representation. The state derivative equation is uniform in time and given in a descriptor form in (2), similar to [2][4][5]. The choice of model outputs, such as air outlet temperature, or evaporation pressure, will depend on the interface with other system component models.

$$x_e = \begin{bmatrix} \zeta_{e1} & P_e & h_{e2} & T_{e1w} & T_{e2w} & \overline{\gamma}_e \end{bmatrix}^T \tag{1}$$

$$Z_e(x_e, u_e)\dot{x}_e = f_e(x_e, u_e) \tag{2}$$

1) Governing Equations (two-zone representation)

The governing equations for the refrigerant-side model of each control volume (two-phase/superheat zone) are formulated in (5) based on the principles of mass and energy conservation. An important mean void fraction equation is included for model switching consideration [2].

Two additional state equations are given in (3) and (4) using average wall temperature in each zone as a state variable.

$$\frac{dT_{e1w}}{dt} = \frac{1}{\zeta_{e1}}\left[\frac{-\dot{Q}_{e1R} - \dot{Q}_{e1A}}{(mc)_{ew}} + (T_{e1wt} - T_{e1w})\frac{d\zeta_{e1}}{dt}\right] \tag{3}$$

$$\frac{dT_{e2w}}{dt} = \frac{1}{\zeta_{e2}}\left[\frac{-\dot{Q}_{e2R} - \dot{Q}_{e2A}}{(mc)_{ew}} + (T_{e2w} - T_{e1wt})\frac{d\zeta_{e1}}{dt}\right] \tag{4}$$

$$\begin{bmatrix} 1 & -\frac{\zeta_{e2}}{\rho_{e2}}\frac{\delta\rho_{e2}}{\delta P_e} & -\frac{\zeta_{e2}}{\rho_{e2}}\frac{\delta\rho_{e2}}{\delta h_{e2}} & 0 & \frac{1}{\rho_{e2}V_{eR}} \\ 0 & -\frac{1}{\rho_{e2}} & 1 & 0 & -\frac{h_{eg}-h_{e2}}{\rho_{e2}V_{eR}\zeta_{e2}} \\ 1 & \frac{\zeta_{e1}}{\rho_{e1}}\frac{\delta\rho_{e1}}{\delta P_e} & 0 & \frac{\zeta_{e1}}{\rho_{e1}}\frac{\delta\rho_{e1}}{\delta\overline{\gamma}_e} & \frac{1}{\rho_{e1}V_{eR}} \\ 0 & \frac{\delta h_{e1}}{\delta P_e} - \frac{1}{\rho_{e1}} & 0 & \frac{\delta h_{e1}}{\delta\overline{\gamma}_e} & \frac{h_{eg}-h_{e1}}{\rho_{e1}V_{eR}\zeta_{e1}} \\ 0 & \frac{\delta\overline{\gamma}_{etot}}{\delta P_e} & 0 & -1 & 0 \end{bmatrix} \begin{bmatrix} \frac{d\zeta_{e1}}{dt} \\ \frac{dP_e}{dt} \\ \frac{dh_{e2}}{dt} \\ \frac{d\overline{\gamma}_e}{dt} \\ \dot{m}_{e12} \end{bmatrix} = \begin{bmatrix} \frac{\dot{m}_{eoR}}{\rho_{e2}V_{eR}} \\ \frac{\dot{Q}_{e2R} - \dot{m}_{eoR}(h_{e2} - h_{eg})}{\rho_{e2}V_{eR}\zeta_{e2}} \\ \frac{\dot{m}_{einR}}{\rho_{e1}V_{eR}} \\ \frac{\dot{Q}_{e1R} + \dot{m}_{einR}(h_{ein} - h_{e1})}{\rho_{e1}V_{eR}\zeta_{e1}} \\ K_e(\overline{\gamma}_e - \overline{\gamma}_{etot}) \end{bmatrix} \tag{5}$$

In (3) and (4), the heat transfer rates from the heat exchanger structure to the external air and internal refrigerant in each control volume are calculated from (6) and (7), respectively.

$$\dot{Q}_{eiA} = \zeta_{ei}\dot{m}_{eA}c_{ePA}(T_{eoiA} - T_{einA}) \tag{6}$$

$$\dot{Q}_{eiR} = \zeta_{ei}U_{eiR}A_{eSR}(T_{eiw} - T_{eiR}) \tag{7}$$

2) Governing Equations (one-zone representation)

In a one-zone evaporator model representation, the superheat zone becomes inactive, and the constant length of two-phase zone is described by:

$$\frac{d\zeta_{e1}}{dt} = 0 \tag{8}$$

The governing equations for the refrigerant-side of the two-phase zone become:

$$\begin{bmatrix} \frac{\zeta_{e1}}{\rho_{e1}}\frac{\delta\rho_{e1}}{\delta P_e} & \frac{\zeta_{e1}}{\rho_{e1}}\frac{\delta\rho_{e1}}{\delta\overline{\gamma}_e} \\ \frac{\delta h_{e1}}{\delta P_e} - \frac{1}{\rho_{e1}} & \frac{\delta h_{e1}}{\delta\overline{\gamma}_e} \end{bmatrix} \begin{bmatrix} \frac{dP_e}{dt} \\ \frac{d\overline{\gamma}_e}{dt} \end{bmatrix} = \begin{bmatrix} \frac{\dot{m}_{einR} - \dot{m}_{eoR}}{\rho_{e1}V_{eR}} \\ \frac{\dot{Q}_{e1R} + \dot{m}_{einR}(h_{ein} - h_{e1}) - \dot{m}_{eoR}(h_{eo} - h_{e1})}{\rho_{e1}V_{eR}\zeta_{e1}} \end{bmatrix} \tag{9}$$

Two *pseudo-state* equations, introduced in (10) and (11), represent the refrigerant enthalpy and wall temperature dynamics, respectively, for the superheat zone. Equations (10) and (11), along with (3), (8), and (9), ensure that the one-zone evaporator model shares the same dynamic state vector in (1) as the two-zone model of (3), (4), and (5).

$$\frac{dh_{e2}}{dt} = K_{eh}(h_{eg} - h_{e2}) \tag{10}$$

$$\frac{dT_{e2w}}{dt} = K_{ew}(T_{e1w} - T_{e2w}) \tag{11}$$

The *pseudo-state* equations in (10) and (11) are similar to latent tracking approaches in bumpless transfer systems. In effect, the states of the inactive superheat zone are forced to track the corresponding states of the active zone so as to maintain similarity when the occasion occurs to switch back to the two-zone model.

3) Switching criteria for evaporator model

Switched system approaches given in [2] are used as guidelines to choose the appropriate criteria for switching the evaporator model between different representations. Specifically, the evaporator model representation switches from two zones to one zone when the refrigerant in the evaporator does not absorb enough heat to change phase (i.e. the superheat region disappears). Mathematically, this switching condition is defined as:

$$1-\zeta_{e1}=\zeta_{e2}<\zeta_{e\min} \quad and \quad \frac{d\zeta_{e1}}{dt}>0 \tag{12}$$

where $\zeta_{e\min}$ is a tunable parameter [2].

The one-zone switches to the two-zone model when

$$\overline{\gamma}_e-\overline{\gamma}_{etot}>0 \quad and \quad \frac{d\overline{\gamma}_e}{dt}>0 \tag{13}$$

The switch condition in (13) is based on void fraction [2] and can be described as, 'existence and further increase of excess vapor in two-phase zone indicates the occurrence of superheat zone in evaporator.'

B. Extended Switched Condenser Model

The switched condenser model in [2] was very limited in its capabilities. To enable modeling of full *stop-start* cycles requires additional configurations of the system states. Here, the switched condenser model of [2] is extended to consist of five different model representations. These five *modes* are given in Fig. 2.

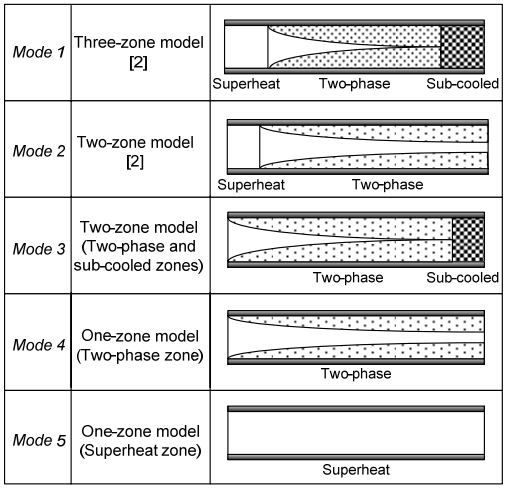

Fig. 2. Switched moving-boundary condenser model structure

Under nearly all steady state conditions, the refrigerant entering the condenser is a superheated vapor. For a single *stop-start* cycle, either *mode 1* or *mode 2* [2] becomes the initial and/or final state in the condenser model. The other three *modes* are intermediate conditions during transients.

The condenser conditions at each time instant are described by a uniform dynamic state vector:

$$x_c=\begin{bmatrix}h_{c1} & P_c & h_{c3} & \zeta_{c1} & \zeta_{c2} & T_{c1w} & T_{c2w} & T_{c3w} & \overline{\gamma}_c\end{bmatrix}^T \tag{14}$$

This implies that the *pseudo-state* equations are included in all condenser model representations; except *mode 1* which has all three zones active already. Additional details about switching between *mode 1* and *mode 2* representations can be found in [2].

1) Mode 3 (two-zone representation)

The condenser model is represented as a two-zone (two-phase and sub-cooled zones) representation in this mode. A switch could occur from *mode 1* to *mode 3* when the superheat zone length approaches 0. The inlet refrigerant is assumed to be saturated vapor in this representation. The governing equations for each control volume on the refrigerant-side of the heat exchanger are derived by applying the laws of mass and energy conservation as in (15).

$$\begin{bmatrix}1 & 0 & -\frac{\zeta_{c3}}{\rho_{c3}}\frac{\delta\rho_{c3}}{\delta h_{c3}} & 0 & \frac{1}{\rho_{c3}V_{cR}}\\ 0 & -\frac{1}{\rho_{c3}} & 1 & 0 & -\frac{h_{cf}-h_{c3}}{\rho_{c3}V_{cR}\zeta_{c3}}\\ 1 & \frac{\zeta_{c2}}{\rho_{c2}}\frac{\delta\rho_{c2}}{\delta P_c} & 0 & \frac{\zeta_{c2}}{\rho_{c2}}\frac{\delta\rho_{c2}}{\delta\gamma_c} & \frac{1}{\rho_{c2}V_{cR}}\\ 0 & \frac{\delta h_{c2}}{\delta P_c}-\frac{1}{\rho_{c2}} & 0 & \frac{\delta h_{c2}}{\delta\overline{\gamma}_c} & \frac{h_{cf}-h_{c2}}{\rho_{c2}V_{cR}\zeta_{c2}}\\ 0 & \frac{\delta\overline{\gamma}_{ctot}}{\delta P_c} & 0 & -1 & 0\end{bmatrix}\begin{bmatrix}\frac{d\zeta_{c2}}{dt}\\ \frac{dP_c}{dt}\\ \frac{dh_{c3}}{dt}\\ \frac{d\overline{\gamma}_c}{dt}\\ \dot{m}_{c23}\end{bmatrix}=\begin{bmatrix}\frac{\dot{m}_{coR}}{\rho_{c3}V_{cR}}\\ \frac{\dot{Q}_{c3R}}{\rho_{c3}V_{cR}\zeta_{c3}}\\ \frac{\dot{m}_{cinR}}{\rho_{c2}V_{cR}}\\ \frac{\dot{Q}_{c2R}+\dot{m}_{cinR}(h_{cg}-h_{c2})}{\rho_{c2}V_{cR}\zeta_{c2}}\\ K_c(\overline{\gamma}_c-\overline{\gamma}_{ctot})\end{bmatrix} \tag{15}$$

If the superheat zone is made inactive we use

$$\frac{d\zeta_{c1}}{dt}=0 \tag{16}$$

and the state equation for refrigerant enthalpy in the superheat zone is as follows:

$$\frac{dh_{c1}}{dt}=0.5\frac{dh_{cin}}{dt}+0.5\frac{\delta h_{cg}}{\delta P_c}\frac{dP_c}{dt} \tag{17}$$

State equations for the average wall temperature in each control zone are similar to those in *mode 1* [2], except the following *pseudo-state* equation governs the wall behavior in the inactive superheat zone:

$$\frac{dT_{c1w}}{dt}=K_{cw}(T_{c2w}-T_{c1w}) \tag{18}$$

2) Mode 4 (one-zone representation)

When the sub-cooled zone length in *mode 3*, or the superheat zone length in *mode 2*, is nearly zero, the condenser will switch to the two-phase zone model representation given by *mode 4*. The governing equations for the refrigerant-side are analogous to (9) in the one-zone evaporator model. The same *pseudo-state* equations from *mode 2* [2] are used to handle the inactive sub-cooled zone, while state equations (16), (17) and (18) still apply.

3) Mode 5 (one-zone representation)

Specific attention must be paid to *mode 5*, the superheat zone condenser model representation. *Modes* could switch from *4* to *5* for certain conditions during a shut-down transient as will be seen in Section III. An alternate state defined as *'uniform superheat enthalpy'* (h_{c1alt}) is used in this model representation. This means the refrigerant in *mode 5* has the same enthalpy throughout the condenser. This differs from the general definition of refrigerant enthalpy for a superheated zone as given in [5]. The initial condition for h_{c1alt} upon initiating *mode 5* is the refrigerant saturated vapor enthalpy.

Using mass and energy conservation laws, the differential equations for the refrigerant are:

$$\begin{bmatrix}\frac{\delta\rho_{c1}}{\delta P_c} & \frac{\delta\rho_{c1}}{\delta h_{c1alt}}\\ -\frac{1}{\rho_{c1}} & 1\end{bmatrix}\begin{bmatrix}\frac{dP_c}{dt}\\ \frac{dh_{c1alt}}{dt}\end{bmatrix}=\begin{bmatrix}\frac{\dot{m}_{cinR}-\dot{m}_{coR}}{\zeta_{c1}V_{cR}}\\ \frac{\dot{Q}_{c1R}+\dot{m}_{cinR}(h_{cin}-h_{c1alt})-\dot{m}_{coR}(h_{co}-h_{c1alt})}{\rho_{c1}V_{cR}\zeta_{c1}}\end{bmatrix} \tag{19}$$

State equations like (16) are used to represent a constant length of superheat and an inactive two-phase zone. *Pseudo-*

state equations similar to [2] are used for modeling average wall temperatures and enthalpies in inactive zones and are applied here in *mode 5*. Additionally, the mean void fraction state equation is now described as:

$$\frac{d\bar{\gamma}_c}{dt} = K_c(1-\bar{\gamma}_c) \tag{20}$$

4) Switching criteria for extended switched condenser

As mentioned in [2], conservation of refrigerant mass is the major concern when choosing the switching criterion between different model representations. Considering there are five *modes* in the switched condenser model, there are many possibilities for switching scenarios during *stop-start* cycle dynamics depending on the different VCC operating conditions. Table I presents the choices of switching criteria between different *modes* used in the following. These are chosen because they are relevant to particular model validation data used in Section III. Other possible switching conditions between certain *modes* in condenser could easily be incorporated without loss of generality.

TABLE I
SWITCHING CONDITION IN CONDENSER

Before Switch	After Switch	Switching Condition
mode 1	*mode 2*	[2]
mode 1	*mode 2*	$h_{co} > h_{cf}$ *and* $\frac{dh_{c3}}{dt} > 0$
mode 1	*mode 3*	$\zeta_{c1} < \zeta_{c\min}$ *and* $\frac{d\zeta_{c1}}{dt} < 0$
mode 2	*mode 4*	$\zeta_{c1} < \zeta_{c\min}$ *and* $\frac{d\zeta_{c1}}{dt} < 0$
mode 3	*mode 4*	$\zeta_{c3} < \zeta_{c\min}$ *and* $\frac{d\zeta_{c2}}{dt} > 0$
mode 4	*mode 5*	$\bar{\gamma}_c > 1$ *and* $\frac{d\bar{\gamma}_c}{dt} > 0$
mode 5	*mode 2*	$\Delta\zeta_c > \zeta_{c\min}$ *and* $\frac{dh_{co}}{dt} < 0$
mode 2	*mode 1*	[2]

In [2], the authors define a relevant switching scheme between *mode 1* and *mode 2* and support the switching conditions with simulation examples. Another condition for the switching from *mode 1* to *mode 2* can be stated as, 'the outlet refrigerant condition becomes a vapor-liquid mixture and the refrigerant enthalpy is increasing.' The mean void fraction in the condenser determines the switch from *mode 4* to *mode 5*. In start-up operation, one switch routine is from the one-zone (superheat zone) *mode 5* model to the two-zone (superheat and two-phase zones) *mode 2* model. The switch is triggered when 'a prescribed amount of vapor-liquid mixture is noticeable and continuing to accumulate in the one-zone (superheat) condenser model.' The normalized length of vapor-liquid mixture in (21) is calculated in each time instant based on the refrigerant mass conservation principle. $\zeta_{c\min}$'s value is user defined.

$$\Delta\zeta_c = \frac{\rho_{c1alt}\zeta_{c1}V_{cR} - M_{cR}}{\rho_{c1alt}V_{cR} - \rho_{c2alt}V_{cR}} \tag{21}$$

III. MODEL VALIDATION

A. Simulation Environment

To validate the framework introduced in Section II, the switched heat exchanger models described above are implemented in Thermosys, a MATLAB toolbox for simulating and analyzing the behavior of vapor compression cycle systems [9]. A particular vapor compressor cycle system is modeled in Thermosys to simulate *stop-start* cycle dynamics. The system includes a compressor, an electronic expansion valve, switched heat exchangers, and pipe models connecting each component. The compressor and expansion valve mass flow models are developed with semi-empirical modeling approaches [10].

Refrigerant-side and air-side heat transfer coefficients are computed separately for the switched heat exchanger models. The air-side heat transfer coefficients are calculated by *j*-factor correlations [11]. Empirical equations are used for refrigerant heat transfer coefficient calculation in the two-phase zones. A *Colburn modulus-Reynolds number* correlation is used for refrigerant heat transfer coefficient calculation in superheat and sub-cooled zones. All the heat transfer coefficients are updated during the cycle dynamics simulation. Further details on solution procedures for switched heat exchangers are found in [2].

B. Experimental System

A schematic of the experimental system in validation configuration is given in Fig. 3. Physical parameters and more detailed descriptions about the experimental system's components can be found in [12].

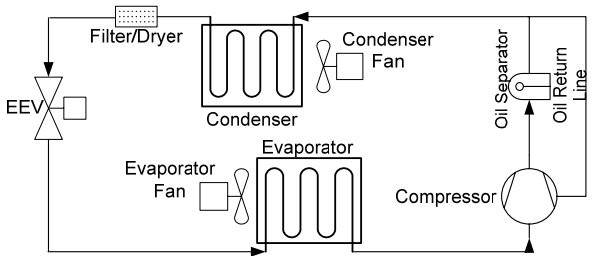

Fig. 3. Schematic of the experimental system

C. Model Validation Results

The validation test scenario includes *stop-start* step changes in compressor speed, whilst fixing the other three inputs: valve opening, condenser/evaporator air mass flow rate. This is summarized in Table II along with condenser/ evaporator air inlet temperature. Fig. 4 displays the dynamic switching of different *modes* in the condenser during these particular *stop-start* transients. The plots in Fig. 5 to Fig. 8 compare experimental data with variable system outputs. Despite some quantitative discrepancies, the qualitative agreement is quite good.

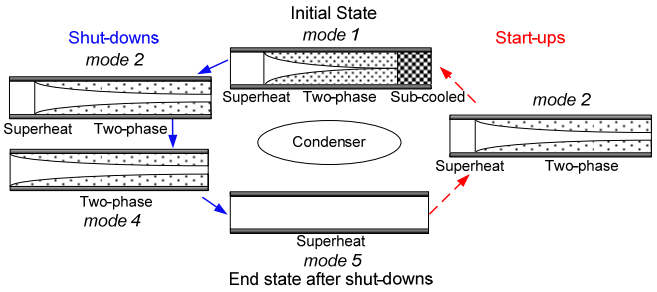

Fig. 4. Switching schemes of different modes in Condenser

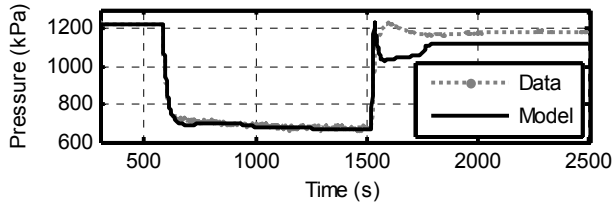

Fig. 5. Condenser pressure

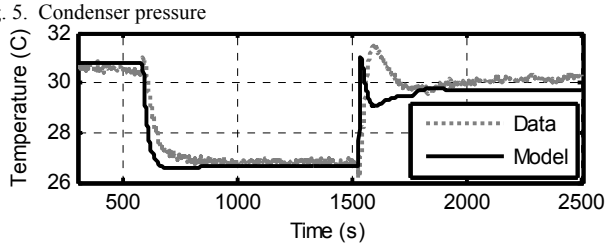

Fig. 6. Condenser air outlet temperature

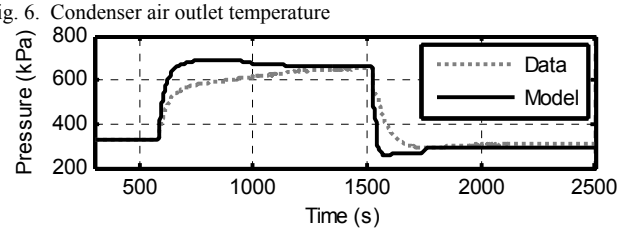

Fig. 7. Evaporator pressure

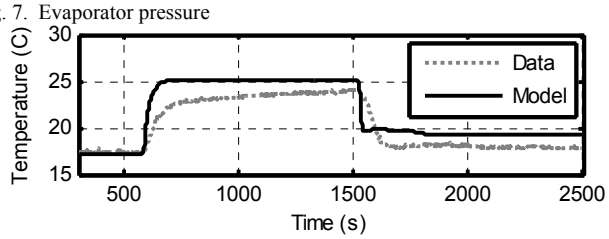

Fig. 8. Evaporator air outlet temperature

TABLE II
SYSTEM INPUTS

Input	Step Time for Shut-down	Before Shut-down	Step Time for Start-up
Compressor speed	585s	1500 rpm	1522s
EEV opening	11%		
Cond. air mass flow rate	0.2996 kg/s		
Evap. air mass flow rate	0.14 kg/s		
Cond. air inlet temperature	26.6°C		
Evap. air inlet temperature	25.1°C		

IV. A CASE STUDY IN STOP-START CYCLE DYNAMICS

Here we use the previously developed model in a full cycle case study to illustrate its potential uses and benefits. *Stop-start* cycle operations are a common method of operating VCC systems in the HVAC industry. Presented in Section II and III, a validated dynamic VCC model system with *stop-start* cycle capabilities has been developed. With the switched heat exchanger models, the VCC system handles the transition dynamics between full refrigerant flow, no flow and back to full flow. This provides practitioners in the HVAC industry with a key tool to use in control design development.

This section is divided into two parts. First a validated dynamic environmental model is introduced to act as a load to the VCC. Secondly, we couple this environmental load model to the VCC model and simulate the combined system with an industry standard controller.

A. Environmental Load Model

1) Load Model Descriptions

The environmental load model is developed based on a heat balance (HB) processing method [13]. Fig. 9 portrays the load model structure. The time varying model inputs are ambient temperature, supply air mass flow rate, and supply air temperature. The environment load model will couple to the VCC model such that the load model inputs, e.g. supply air temperature, are the outputs of the VCC model, e.g. evaporator outlet air temperature. Similarly, the VCC model inputs, e.g. evaporator inlet air temperature, will be the load model outputs, e.g. return air temperature. The dynamic state vector is given in (22). Simplifying model assumptions are:

1) Uniform air temperature with well-mixed air in the enclosed environmental zone.
2) Uniform surface temperature for the enclosed environment including its inside and outside wall surface.
3) One dimensional heat conduction through zone walls.

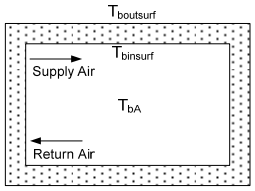

Fig. 9. Environmental load model structure

$$x_b = \begin{bmatrix} T_{bA} & T_{binsur} & T_{bosur} \end{bmatrix}^T \tag{22}$$

The governing equations are obtained by applying energy conservation principles as follows:

$$\frac{dT_{bA}}{dt} = \frac{\dot{Q}_{bincon} - \dot{Q}_{cap}}{(mc)_{bA}} \tag{23}$$

$$\frac{dT_{binsur}}{dt} = \frac{\dot{Q}_{bcond} - \dot{Q}_{bincon}}{(mc)_{bwall}} \tag{24}$$

$$\frac{dT_{bosur}}{dt} = \frac{\dot{Q}_{bocon} - \dot{Q}_{bcond}}{(mc)_{bwall}} \tag{25}$$

The heat flow from the environment's inside wall surface to the air inside the environment is given in (26). The heat flow from the environment's outside wall surface to the ambient air is given in (27). Equations (26) and (27) are both based on convective heat transfer. The heat flow from the environment's outside wall surface to its inside wall

surface is based on conduction and is given in (28). The VCC system capacity is defined in (29). Convective heat transfer coefficients, including forced and free convection in the enclosed environment, are calculated using empirical equations [14][15].

$$\dot{Q}_{bincon} = H_{bincon} A_{binsur} (T_{binsur} - T_{bA}) \quad (26)$$

$$\dot{Q}_{bocon} = H_{bocon} A_{bosur} (T_{amb} - T_{bosur}) \quad (27)$$

$$\dot{Q}_{bocon} = (UA)_{bwall} (T_{bosur} - T_{binsur}) \quad (28)$$

$$\dot{Q}_{cap} = \dot{m}_A c_{PA} (T_{bA} - T_{\sup}) \quad (29)$$

2) Load Model Validation

The load model is implemented in Thermosys [9]. The model validation scenario involves a temperature pull-down and control test for the enclosed environmental zone. The test was done within an industrial test unit at Thermo King Corporation.

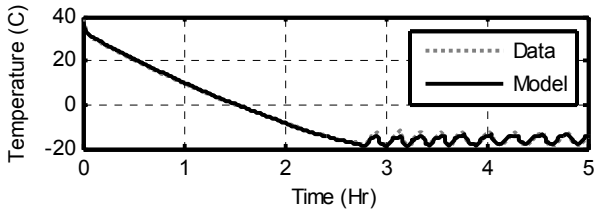

Fig. 10. Return air temperature

The test procedure can be described as: "Pull-down the enclosed zone air temperature from ambient temperature to a given setpoint using the refrigeration system; then run *stop-start* cycle operations to maintain the temperature." Comparison of return air temperature from test data and model output is presented in Fig. 10.

B. Hysteretic Control in VCC/Environment System

As indicated in Fig. 10, *stop-start* cycles are often used in industry to maintain temperature setpoints for VCC systems. The control strategy is usually a simple hysteresis. Fig. 11 describes the principle of hysteretic control. Two kinds of control actions are considered for simplicity: ON - high compressor speed; OFF - zero compressor speed. Either control action is driven by the error between measured temperature and temperature set-point in the enclosed environmental zone. Control engineers have the flexibility to determine the width of the hysteresis. Additionally, an offset is often applied such that the hysteresis is not symmetric about zero error.

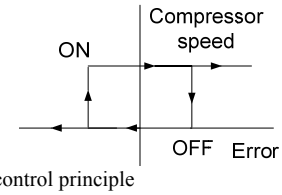

Fig. 11. Hysteretic control principle

To demonstrate the utility of the modeling approach, a combined VCC/Environment system, including a vapor compressor cycle and environmental load model, were constructed in Thermosys to simulate system behaviors with hysteretic temperature controller. The desired temperature in the enclosed environmental zone is set to be 5°C with on/off hysteresis switches set to +2 /-1°C. The ambient temperature is 30°C. The switched moving-boundary condenser and evaporator models described in Section II, as well as a compressor and electronic expansion valve model [10], are used in the VCC system. The schematic of simulation system is shown in Fig. 12. One of the VCC system outputs, evaporator air outlet temperature, is used as one of the environmental load model inputs, supply air temperature, while return air temperature from the load model outputs feeds as an input to the VCC system.

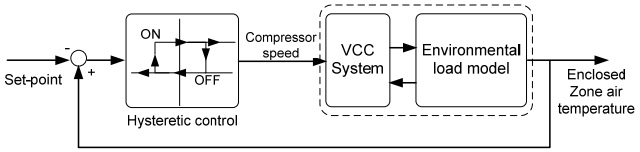

Fig. 12. Schematic of simulation VCC/Environment system

Results for the environment's zone air temperature (return air temperature) and supply air temperature are presented in Fig. 13. Fig. 14 illustrates the control actions of the hysteretic algorithm in terms of compressor speed.

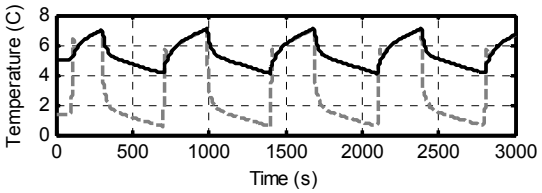

Fig. 13. Input and output plots in the environmental load model; supply air temperature='--', return air temperature='-'

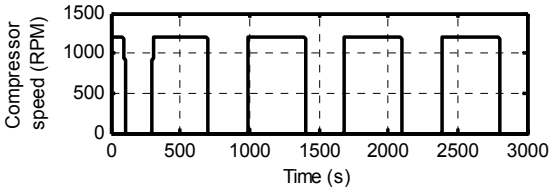

Fig. 14. Control actions in compressor speed

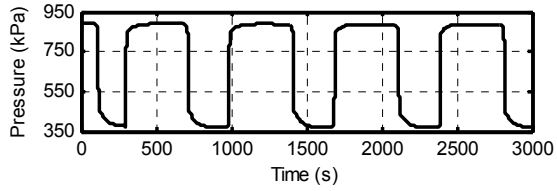

Fig. 15. Condenser pressure

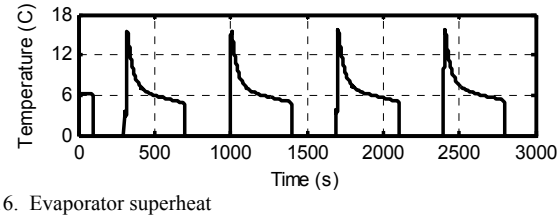

Fig. 16. Evaporator superheat

The plots from Fig. 15 to Fig. 16 present the VCC system performance under these *stop-start* cycle operations. The results provide the practicing HVAC control designer with a great deal of flexibility. S/he can now rapidly adjust

hysteresis setpoints in simulation to narrow down potential choices before moving to expensive test-cell experiments. S/he can examine robustness to varying truck/trailer environmental conditions (e.g. insulation variation), varying ambient conditions (e.g. solar load or ambient temperature profiles), and varying power costs to run the compressor using existing controller frameworks. Equally important is the new opportunity to test advanced controller designs [1] in software and hardware-in-the-loop.

V. Conclusion

To the knowledge of the authors, this paper presents the first moving-boundary dynamic VCC model that captures compressor *stop-start* cycling dynamics. The new moving-boundary heat exchanger models are developed with switched model representations to accommodate the varying numbers of fluid regions during *stop-start* transients. Model validation results are presented that prove the switched heat exchanger models are capable of representing the system cycling behaviors.

A case study in *stop-start* cycling operations with the VCC system is described. First, a dynamic environmental load model is created and validated. Then, simulation results are given for an industry standard hysteretic temperature controller using the combined VCC and environment system. This gives a clear indication of the value of the modeling tools developed for controller development and *in-silico* testing. Future work involves the investigation of the switched VCC/Environment system stability with a set of system and controller parameter variations.

Nomenclature

Variables

A	Area	T	Temperature
c	Specific heat	U	Overall heat transfer coef.
H	Convective coef.	(UA)	Lumped heat transfer coef.
h	Refrig. enthalpy	u	Controllable input
K	Gain; set to 5 s^{-1}	V	Volume
M	Mass	x	State vector
$\dot{m}$	Mass flow rate	$\dot{x}$	Derivative of state vector
(mc)	Thermal capacitance	Z	Coefficient matrix
P	Pressure	$\bar{\gamma}$	Mean void fraction
$\dot{Q}$	Heat transfer rate	ρ	Average refrig. density
ζ	Fraction of heat exchanger length covered by zone		
$\Delta\zeta$	Normalized length of excess vapor-liquid mixture		

Subscripts

A	Air	*insur*	Inside surface
alt	Alternative	j	Zone number
amb	Ambient	min	Minimum before switches
b	Environmental load	*ocon*	Outside-surface convection
c	Condenser	*osur*	Outside surface
cap	VCC system capacity	o	Outlet
cond	Conduction	*PA*	Air at constant pressure
e	Evaporator	R	Refrigerant
f	Saturated liquid	sup	Supply air
g	Saturated vapor	*SR*	Refrig.-to-structure surface
h	*Pseudo-state* enthalpy	w	Heat exchanger structure
in	Inlet	*wall*	Wall in environmental load
incon	Inside-surface convection	*wt*	Transported structure temp.
cj	Superheat, two-phase, sub-cooled zone in Condenser		
*c*23	Interface between two-phase and sub-cooled zone		
ej	Two-phase, superheat zone in Evaporator		
*e*12	Interface between two-phase and superheat zone		
tot	Complete condensation/evaporation		

Acknowledgement

This work was supported in part by the sponsoring companies of the Air-Conditioning and Refrigeration Center at the University of Illinois at Urbana-Champaign and Thermo King Corporation.

References

[1] Bendapudi, S., and Braun, J. E., "A Review of Literature on Dynamic Models of Vapor Compression Equipment," *ASHRAE Report,* No. 4036-5.

[2] McKinley, T. L., Alleyne, A. G., "An Advanced Nonlinear Switched Heat Exchanger Model for Vapor Compression Cycles Using the Moving-Boundary Method," *International Journal of Refrigeration*, vol. 31, pp. 1253-1264, 2008.

[3] Rasmussen, B. P., Musser, A., Alleyne, A. G., "Model-Driven System Identification of Transcritical Vapor Compression Systems," *IEEE Trans on Control Systems Technology*, vol. 13, pp. 444-451, 2005.

[4] Alleyne, A. G., Rasmussen, B. P., Keir, M. C., Eldredge, B. D., "Advances in Energy Systems Modeling and Control," *Proc of the 2007 Am Control Conf*, New York, NY USA, pp. 4363-4373.

[5] Rasmussen, B. P., "Dynamic Modeling and Advanced Control of Air Conditioning and Refrigeration Systems," PhD. Dissertation, Dept. of Mechanical Engineering, University of Illinois at Urbana-Champaign, 2005.

[6] Eldredge, B. D., "Improving the Accuracy and Scope of Control-Oriented Vapor Compression Cycle System Models," MS Thesis, Dept. of Mechanical Engineering, University of Illinois at Urbana-Champaign, 2006.

[7] Dhar, M., Soedel, W., "Transient Analysis of a Vapor Compression Refrigeration System," *Proceedings of the 15th International Congress of Refrigeration,* Venice, vol. 2, pp. 1031-1067, 1979.

[8] Willatzen, M., Pettit, N.B.O.L., Ploug-Sorensen, L., "A General Dynamic Simulation Model for Evaporators and Condensers in Refrigeration. Part I: Moving-Boundary Formulation of Two-Phase Flows With Heat Exchange," *Int J Refrigeration,* Vol. 21, No. 5, pp. 398-403, 1998.

[9] Rasmussen, B. P., "Control-Oriented Modeling of Transcritical Vapor Compression Systems," MS Thesis, Dept. of Mechanical Engineering, University of Illinois at Urbana-Champaign, 2002.

[10] Rasmussen, B. P., Alleyne, A. G., "Control-Oriented Modeling of Transcritical Vapor Compression Systems," *Journal of Dynamic Systems, Measurement, and Control*, vol. 126, pp. 54-64, 2004.

[11] Kays, W. M., London, A. L., *Compact Heat Exchangers*, McGraw-Hill, Inc., New York, 1984.

[12] Keir, M. C., Alleyne, A. G., "Feedback Structures for Vapor Compression Cycle Systems," *Proc of the 2007 Am Control Conf*, New York, NY USA, pp. 5052-5058.

[13] ASHRAE, ASHRAE Handbook: Fundamentals (SI Edition), Chapter 30, Atlanta, GA: American Society of Heating, Refrigerating, and Air-Conditioning Engineers, 2005.

[14] McAdams, W. H., *Heat Transmission*, McGraw-Hill, Inc., New York, 1954.

[15] Musy, M., Wurtz, E., Winkelmann, F., Allard, F., "Generation of a Zonal Model to Simulate Natural Convection in a Room with a Radiative/Convective Heater," *Building and Environment*, vol. 36, pp. 589-596, 2001.

[16] Hencey, B., Jain, N., Li, B., Alleyne, A. G., "Decentralized Feedback Structures of a Vapor Compression System," *Proceedings of the 2008 ASME DSCC*, Ann Arbor, MI, October 20-22, 2008.